

Photocurrent Generation in a Silicon Waveguide Integrated with Periodically Interleaved P-N Junctions

Haike Zhu, Linjie Zhou*, Xiaomeng Sun, Jingya Xie, Zhi Zou, Liangjun Lu, Xinwan Li, and Jianping Chen

State Key Laboratory of Advanced Optical Communication Systems and Networks, Department of Electronic Engineering, Shanghai Jiao Tong University, Shanghai 200240, P. R. China

*ljzhou@sjtu.edu.cn

Abstract

We investigate the photocurrent generation in a silicon waveguide embedded with interleaved p-n junctions. Due to the surface-state absorption and the high built-in electrical-field, the responsivity reaches ~ 14.9 mA/W and the bandwidth is 11.5 GHz.

I. INTRODUCTION

Integrated silicon photonics has seen a rapid development in recent years [1]. As a key component in silicon photonics, photodetector is still very challenging and leaves a lot of work to do for researchers [2]. Silicon has an indirect bandgap of 1.12 eV, which is not suitable for photodetection in the near-infrared telecom wavelengths. A. J. Reddy *et al.* studied the defect states of the silicon surface [3], indicating that the bandgap on the silicon surface is much lower than that of the bulk silicon due to the interruption of the periodic potential at the surface [2]. Recently, all-silicon photodetectors based on the surface-state absorption (SSA) effect have been demonstrated with a responsivity of 0.12 mA/W [4].

Although the responsivity of all-silicon photodetectors based on the SSA effect at the telecom wavelength is low compared to other photocurrent generation mechanisms such as mid-bandgap absorption (MBA) [5], it is very easy and convenient to generate photocurrent, as long as there is an overlap between waveguide surface and optical field. Thus, such all-silicon photodetectors can be used for on-chip optical power monitoring. F. Logan *et al.* theoretically investigated the relationship between the photocurrent and the separation of the P^+/N^+ contacts [6]. Their studies show that the stronger the electrical field is, the higher the photocurrent is. Combining these two factors together, we can collect much more photocurrent generated by the SSA effect.

In this paper, we propose and experimentally demonstrate an all-silicon photodetector constituted by a silicon waveguide embedded with periodically interleaved p-n junctions. For comparison, we also characterize the photocurrent generation in a p-i-n junction embedded silicon waveguide fabricated in the same run as a reference.

II. DEVICE STRUCTURE

Fig. 1(a) shows the schematic of our proposed all-silicon photodetector. The cross-sectional dimension of

the silicon waveguide is $400 \text{ nm} \times 220 \text{ nm}$ with a slab height of 60nm. Periodically lightly doped P⁻ and N⁻ regions are across the silicon waveguide with a width of $W_d = 1 \text{ }\mu\text{m}$ and a length of $L_d = 0.6 \text{ }\mu\text{m}$. The doping concentrations are $\sim 10^{17} \text{ cm}^{-3}$. Beside the P⁻/N⁻ doping region is the heavily doped P⁺/N⁺ region with a doping concentration of $\sim 10^{20} \text{ cm}^{-3}$ for ohmic contact with Aluminum metal.

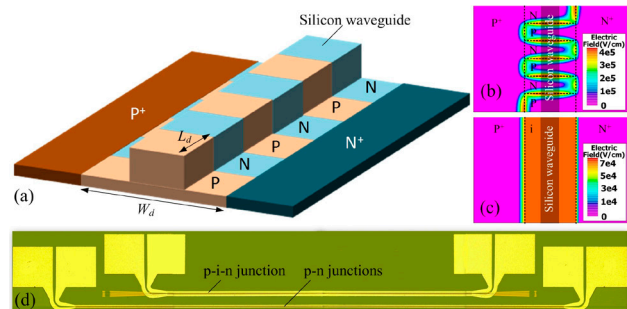


Fig. 1. (a) Schematic of the proposed all-silicon photodetector composed of a straight silicon waveguide embedded with periodically interleaved p-n junctions. (b) Electric field distribution in the slab of proposed device at -10 V bias voltage. (c) Electric field distribution in the reference device based on a p-i-n junction at -10 V bias voltage. (d) Optical microscope image of the proposed and reference silicon photodetectors.

Figs. 1(b) and (c) show the electric field distributions in the straight waveguides embedded with periodically interleaved p-n junctions and a p-i-n junction at the bias of -10 V, respectively. In the reference waveguide, there is no N⁻/P⁻ doping regions and the other parameters are the same. It is quite obvious that the one with the interleaved p-n junctions has a much higher electric field in the depletion region ($\sim 4 \times 10^5 \text{ V/cm}$) than that with the p-i-n junction ($\sim 6 \times 10^4 \text{ V/cm}$). The higher electric field is due to the narrower width of depletion region. This strong electric field gives rise to a high carrier velocity, so that the carrier recombination rate is considerably reduced, resulting in an increased generation of photocurrent.

Fig. 1(d) shows the optical microscope image of the two all-silicon photodetectors. The bottom one is based on 2.2 mm long periodically interleaved p-n junctions and the top one is based on a 1.53 mm long single p-i-n junction. The fabrication process is the same as in our previous work [5].

III. EXPERIMENTAL RESULTS

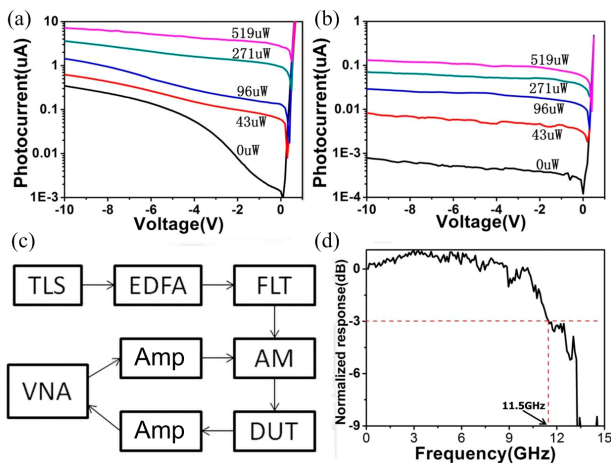


Fig. 2. (a) and (b) Generated photocurrent as a function of bias voltage at various coupled power levels in (a) the proposed device and (b) the reference device. (c) Experimental setup for high speed characterization. TLS: tunable laser source, EDFA: erbium-doped optical fiber amplifier, FLT: filter, AM: amplitude modulator, DUT: device under test, Amp: microwave amplifier, VNA: vector network analyzer. (d) High speed response of the proposed device at the bias voltage of -10V .

We used a tunable laser as the light source. The input light was transverse-electrically (TE) polarized by using a polarize controller. Light was coupled into the waveguide using a lensed fiber with a coupling loss of $\sim 7\text{ dB}$. The photocurrent was collected by using a pair of 40 GHz microwave probes contacting the metal pads of the device. We placed an erbium-doped optical fiber amplifier (EDFA) before the device to boost up the optical power. A 1-nm bandwidth optical filter was used to filter out the ASE noise. In our measurement, we fixed the wavelength at 1550 nm.

Fig. 2(a) shows the measured generated photocurrent as a function of bias voltage at various coupled power levels for our proposed device. As a comparison, Fig. 2(b) shows the measured photocurrent for the reference device. The photocurrent generated by the interleaved p-n junctions is almost 100 times higher than that of the p-i-n junction under the same coupled power level. Moreover, the slope of the lines in Fig. 2(a) is larger than that in Fig. 2(b), indicating that the photocurrent generated by the interleaved p-n junctions is more sensitive to the bias voltage. This is because the electric field increases more in the interleaved p-n junctions when the bias voltage increases. The responsivity of our proposed photodetector is $\sim 14.9\text{ mA/W}$ at the bias of -10 V . In contrast, the responsivity of the reference device is only $\sim 0.2\text{ mA/W}$ at -10 V . Given the difference in their waveguide length, the responsivity per unit length of our proposed device is still > 50 times higher than that of the reference one.

The high carrier velocity also implies that the interleaved p-n junctions could have a high speed response. Fig. 2(c) shows the experimental setup for high speed photodetection measurement. We used the radio frequency/microwave vector network analyzer (VNA) to measure the S_{21} parameter of the device. A 20 GHz microwave amplifier (Amp) was used to amplify the input electrical signal to drive the amplitude modulator (AM). The generated photocurrent was also amplified by

another Amp before feeding back to the VNA. The VNA scans the frequency from 50 MHz to 20 GHz. Fig. 2(d) shows the measured S_{21} curve at the bias voltage of -10 V . The influence of the measurement system is excluded by normalization. The 3-dB bandwidth of the proposed device is 11.5 GHz, which is probably limited by the travelling electrode design. A better phase matching of the optical and microwave signals upon optimization of the travelling electrode could further improve the bandwidth.

IV. CONCLUSIONS

We experimentally investigated the photocurrent generation based on SSA in a waveguide integrated with interleaved p-n junctions. Because the interleaved p-n junctions possess stronger built-in electrical field than the regular p-i-n junction, the SSA effect is greatly enhanced. The measured responsivity of the proposed device reaches $\sim 14.9\text{ mA/W}$ at -10 V bias. The device was also characterized to have a 3 dB bandwidth of 11.5 GHz.

ACKNOWLEDGMENT

This work was supported in part by 973 program (ID2011CB301700), the National Natural Science Foundation of China (NSFC) (61007039, 61001074, 61127016), the Science and Technology Commission of Shanghai Municipality (STCSM) Project (10DJ1400402).

REFERENCES

- [1] Assia Barkai, Yoel Chetrit, Oded Cohen, Rami Cohen, Nomi Elek, Eyal Ginsburg, Stas Litski, Albert Michaeli, Omri Raday, Doron Rubin, Gadi Sarid, and Nahum Izhaky, "Integrated silicon photonics for optical networks [Invited]," *J. Optical Networking*, vol.6, pp.1536-5379, Jan, 2007.
- [2] Maurizio Casalino, Giuseppe Coppola, Mario Iodice, Ivo Rendina and Luigi Sirleto, "Near-Infrared Sub-Bandgap All-Silicon Photodetectors: State of the Art and Perspectives," *Sensors*, vol.10, pp.10571-10600, Nov, 2010.
- [3] A. J. Reddy, J. V. Chan, T. A. Burr, R. Mo, C. P. Wade, C. E. D. Chidsey, J. Michel, and L. C. Kimerling, "Defect states at silicon surfaces," *Physica B*, vol.273, pp.468, Dec, 1999.
- [4] H. Chen, X. Luo, and A. W. Poon, "Cavity-enhanced photocurrent generation by 1.55 μm wavelengths linear absorption in a p-i-n diode embedded silicon microring resonator," *Appl. Phys. Lett.*, vol.95, pp.171111, Oct, 2009.
- [5] Dylan F. Logan, Philippe Velha, Marc Sorel, Richard. M. De La Rue, Andrew P. Knights, and Paul E. Jessop, "Defect-Enhanced Silicon-on-Insulator Waveguide Resonant Photodetector With High Sensitivity at 1.55 μm ," *IEEE Photon. Technol. Lett.*, vol.22, pp.1530-1532, Oct, 2010.
- [6] Dylan F. Logan, Paul E. Jessop, and Andrew P. Knights, "Modeling Defect Enhanced Detection at 1550 nm in Integrated Silicon Waveguide Photodetectors," *J. Lightw. Technol.*, vol.27, pp.930-937, Apr, 2009.
- [7] L. Zhou, J. Xie, L. Lu, Z. Zou, X. Sun, and J. Chen, "Coupled-resonator-induced-transparency in cascaded self-coupled optical waveguide (SCOW) resonators," in *Proc. Conference on Asia Communication and Photonics (ACP2012)*, Guangzhou (China), Nov, 2012, paper Ath4B.